



#### OPEN ACCESS

##### EDITED BY

Bo Li,  
Guangxi University, China

##### REVIEWED BY

Lin Gong,  
Prairie View A&M University,  
United States  
Peijie Li,  
Guangxi University, China  
Zhuangzhi Guo,  
Henan Institute of Engineering, China

##### \*CORRESPONDENCE

Huang Zeyi,  
✉ huangzy@gxed.com

RECEIVED 21 October 2025

REVISED 12 December 2025

ACCEPTED 06 February 2026

PUBLISHED 12 March 2026

##### CITATION

Zeyi H, Xiayang L, Hang Z, Bo L and  
Dongsheng X (2026) Day-ahead  
optimal scheduling of large-scale  
renewable energy bases based on rime  
optimization algorithm.  
*Front. Energy Res.* 14:1729191.  
doi: 10.3389/fenrg.2026.1729191

##### COPYRIGHT

© 2026 Zeyi, Xiayang, Hang, Bo and  
Dongsheng. This is an open-access  
article distributed under the terms of  
the [Creative Commons Attribution  
License \(CC BY\)](https://creativecommons.org/licenses/by/4.0/). The use, distribution or  
reproduction in other forums is  
permitted, provided the original  
author(s) and the copyright owner(s) are  
credited and that the original  
publication in this journal is cited, in  
accordance with accepted academic  
practice. No use, distribution or  
reproduction is permitted which does  
not comply with these terms.

# Day-ahead optimal scheduling of large-scale renewable energy bases based on rime optimization algorithm

Huang Zeyi\*, Li Xiayang, Zhou Hang, Lu Bo and Xu Dongsheng

China Energy Engineering Guangxi Electric Power Design Institute Co., Ltd., Nanning, China

The integration of large-scale renewable energy (RE) poses complex challenges for day-ahead scheduling, characterized by high-dimensional, nonlinear, and tightly constrained optimization problems. Traditional optimization methods often fail to efficiently handle such complexity, leading to suboptimal solutions and high computational costs. Inspired by the growing potential of artificial intelligence (AI) in clean energy systems, this paper introduces an AI-powered scheduling framework based on the Rime Optimization Algorithm (RIME) to address these issues. We develop a high-fidelity Mixed-Integer Nonlinear Programming (MINLP) model that incorporates wind, photovoltaic, hydro, thermal, nuclear, and pumped storage units, with dual objectives of minimizing operating costs and maximizing RE utilization. Leveraging RIME's bio-inspired mechanisms—soft rime search for adaptive exploration and hard rime piercing for escaping local optima—the algorithm demonstrates superior performance in balancing exploration and exploitation. Extensive simulations on a real-world regional energy base (comprising 470+ units) under four operational modes show that RIME achieves a 6%–10% reduction in operating costs, 100% RE utilization, and 10%–15% faster computation compared to benchmark methods. These results highlight RIME's potential as an efficient AI-driven tool for the smart and sustainable management of complex renewable-rich power systems.

##### KEYWORDS

AI, mixed-integer nonlinear programming, multi-energy systems, renewable energy integration, rime optimization algorithm, smart grid scheduling

## 1 Introduction

Guided by the global imperative for carbon neutrality and the sustainable energy transition, the integration of large-scale renewable energy (RE) into power systems has become a critical pathway worldwide (Chen et al., 2020). In this paper, 'new energy generation' refers specifically to wind and photovoltaic power generation, which are characterized by intermittency and uncertainty. In China, under the "dual carbon" goals, the capacity of renewable power generation continues to expand rapidly. Central to this development are multi-energy complementary energy bases, which leverage centralized control and dispatch to achieve efficient long-distance transmission and improved utilization of power channels (Liu et al., 2024). However, the inherent volatility and uncertainty of wind and photovoltaic (PV) power generation pose significant threats to grid stability, including power flow oscillations, if not managed properly (Qiu, 2021).

To address these challenges, modern energy bases combine renewable sources with flexible regulatory resources. This includes harnessing the rapid response of hydropower,

the base-load support and peak-shaving capability of thermal power, and the “peak-shaving and valley-filling” function of pumped storage. Such integration forms a multi-energy complementary system, which operates through a hierarchical dispatch strategy: prioritizing renewable consumption day-ahead, adjusting hydro and thermal output intra-day, and suppressing short-term fluctuations in real-time via energy storage. This approach not only smooths renewable output fluctuations but also enhances overall operational benefits by reducing curtailment and lowering peak-shaving costs.

The energy base studied in this paper represents a complex integrated system with a high penetration of renewables, supported by regulating sources (e.g., hydropower, pumped storage) and base-load/backup sources (e.g., thermal, nuclear power). Through complementarity, it enhances renewable penetration and operational economy while ensuring system security (Zhou et al., 2024). Nevertheless, the high dimensionality, nonlinearity, and multi-constrained nature of its dispatch problem—involving objectives like economy, renewable utilization, and coupled constraints such as cascaded hydropower balance—present formidable optimization challenges (Lu et al., 2023a).

Currently, numerous research studies have been conducted on the energy planning of power systems incorporating hydro, thermal, wind, photovoltaic, and energy storage systems. Reference (Ke, 2023) developed a supply-demand balance analysis model suitable for such hydro-thermal-wind-PV-storage systems, providing guidance for the dispatch analysis of these systems over long time horizons. Reference (Zhang et al., 2023) proposed a distributed robust optimization approach that can effectively mitigate the impacts caused by load curtailment and the uncertainties associated with renewable energy output. An optimal dispatch model was established, incorporating system operational risk assessment and an adjustable-bound uncertainty convex hull. Addressing the challenges arising from the integration of large-scale renewable energy, Reference (Bai et al., 2022) constructed a robust unit commitment model with concentrating solar power plants to overcome the effects of wind power output fluctuations. This model incorporates conditional value-at-risk and constructs a multi-dimensional uncertainty set encompassing temporal, spatial, and interval dimensions. Reference (Ren Jundong Research on Optimization, 2022) starts from the collaborative coupling of new energy units and conducts optimal dispatch for photovoltaic-gas units. Reference (Bai and Shahidehpour, 1996) proposes an improved particle swarm optimization algorithm to address the unit commitment optimization problem of microgrids with energy diversification.

Faced with the instability of renewable energy output, how to ensure the safe and efficient utilization of clean energy is emerging as a key issue for the future development of power systems. However, the unit commitment involving large-scale wind, solar, hydro, thermal, nuclear, energy storage, and pumped storage units must not only consider numerous system constraints but also take into account the characteristics of each generating unit. Although existing intelligent search algorithms can effectively solve this problem, they still suffer from deficiencies such as poor global search capability and weak iterative information sharing ability. Traditional mathematical programming methods, such as Lagrange Relaxation (LR), often face computational bottlenecks

and struggle with non-convex, large-scale MINLP problems. Conventional heuristic algorithms (e.g., Genetic Algorithm (Wong, 1998), Particle Swarm Optimization (Lu et al., 2023b; Ren, 2022), Tabu Search (Wang, 2011)) have been applied to energy dispatch but often suffer from local optima entrapment, slow convergence, parameter sensitivity, and limited handling of strong constraints (Chen et al., 2010). Thus, there is a pressing need for more advanced, efficient, and intelligent optimization algorithms.

In recent years, artificial intelligence (AI) has emerged as a pivotal transformative driver in the energy sector, with metaheuristic algorithms—an AI subfield inspired by natural phenomena—standing out for their exceptional potential in tackling complex high-dimensional optimization problems. Their inherent ability to navigate vast, non-convex solution spaces makes them ideal for renewable-rich power system optimization, where dimensionality often surpasses traditional methods. The recently proposed RIME algorithm (inspired by rime ice growth) excels in this domain with unmatched high-dimensional problem-solving capabilities: its soft rime search operator enables adaptive, gradient-free global exploration to maintain population diversity and avoid premature convergence in ultra-high-dimensional spaces, while the hard rime piercing operator delivers targeted perturbations for escaping local optima traps amplified by high dimensionality. Complemented by robust global search, rapid convergence, strong resilience to parameter sensitivity, and minimal tuning requirements, RIME is uniquely suited for high-dimensional, multimodal, and strongly constrained scenarios.

Despite its proven prowess in high-dimensional optimization, RIME's potential remains untapped in large-scale multi-energy complementary dispatch—especially in scenarios integrating nuclear power operational constraints and detailed pumped storage modeling, both of which introduce additional layers of dimensionality and complexity. This gap presents a valuable opportunity to harness RIME's advanced high-dimensional optimization capabilities, leveraging AI to advance the operation and optimization of sustainable energy systems.

To bridge this gap, this paper proposes an AI-driven day-ahead scheduling framework for large-scale RE-integrated energy bases using the RIME algorithm. The main contributions are summarized as follows:

**Bridging an Algorithmic Gap:** This paper introduces and tailors the RIME algorithm, a promising yet unexplored metaheuristic in this context, to solve the large-scale, multi-energy complementary dispatch problem—specifically incorporating detailed nuclear power constraints and pumped storage modeling.

**A Practical AI-Driven Scheduling Framework:** This paper develops a complete RIME-based optimization framework that translates the complex MINLP scheduling model into a solvable search problem, with explicit mechanisms for high-dimensional exploration, constraint satisfaction, and escape from local optima.

**Rigorous Empirical Validation:** Through comprehensive case studies on a real-world system under multiple operational modes, this paper provides compelling evidence of the framework's practicality, robustness, and superior performance in terms of economic efficiency, renewable integration, and computational tractability compared to conventional methods.

The remainder of this paper is organized as follows: [Section 2](#) constructs the mathematical model of the energy base. [Section 3](#)

details the RIME algorithm and its tailored application to the scheduling problem. Case studies and results analysis are presented in Section 4. Finally, Section 5 concludes the paper.

## 2 Energy base model with large scale new energy

During the day-ahead optimal scheduling phase, the unit commitment status and output scheme for the next day are optimized and calculated based on the load forecast values. The objective function aims to maximize the utilization of renewable energy output in the coordinated dispatch of various energy sources within the energy base, minimize wind and solar curtailment as much as possible, and ultimately achieve the optimal scheduling of the energy base.

During day-ahead scheduling, the predicted output of renewable energy is adopted as the upper limit of output constraints. By applying the objective function, the planned output of renewable energy is made to approach the predicted value, thereby maximizing the utilization of renewable energy output. The goal is to minimize the total power generation cost and unit start-stop cost throughout the period, on the premise of ensuring that the power grid demand and relevant constraints are satisfied (Zhang, 2020; Hua et al., 2010). The specific model is presented as follows.

### 2.1 Objective function

The objective is to minimize the total power generation cost and unit start-stop cost over the entire period, on the premise of ensuring the satisfaction of power grid demand and compliance with operational constraints. The cost of new energy is mainly concentrated in the early-stage construction phase; compared with traditional thermal power units, its operation cost is negligible. Therefore, the objective function only needs to consider the operation cost of traditional thermal power units and the penalty cost for insufficient actual output of wind and photovoltaic power. Its mathematical model is expressed as follows:

$$\min .F = \sum_{t=1}^T \left[ -\delta_f (P_{f,t,z} - P_{f,t,pre}) - \delta_g (P_{g,t,z} - P_{g,t,pre}) + \sum_{i=1}^N [U_{i,t} C_{i,t} + U_{i,t} (1 - C_{i,t-1}) S_i] \right] \quad (1)$$

In the formula:  $F$  denotes the total objective value;  $N$  represents the total number of thermal power units;  $T$  stands for the total number of operating time periods,  $\delta_f$  is the price penalty factor for wind power output deviation,  $\delta_g$  is the price penalty factor for photovoltaic power output deviation;  $P_{f,t,z}$  is the planned wind power output,  $P_{f,t,pre}$  is the predicted wind power output, with the constraint  $P_{f,t,z} \leq P_{f,t,pre}$ ;  $P_{g,t,z}$  is the planned PV power output at time  $t$ ,  $P_{g,t,pre}$  is the predicted PV power output at time  $t$ , with the constraint  $P_{g,t,z} \leq P_{g,t,pre}$ . If  $P_{f,t,z} > P_{f,t,pre}$ , no penalty is imposed,  $\delta_f$  is set to 0; if  $P_{g,t,z} > P_{g,t,pre}$ , no penalty is imposed,  $\delta_g$  is set to 0.  $U_{i,t}$  indicates the status (on/off) of the  $i$ -th thermal power unit at time  $t$ .

The objective function (1) minimizes the total operational cost, comprising thermal generation costs and penalties for under-utilization of wind and PV power. Maximization of renewable energy utilization is achieved through a two-layer mechanism:

The inequalities  $P_{f,t,z} \leq P_{f,t,pre}$  and  $P_{g,t,z} \leq P_{g,t,pre}$  enforce that renewable generation cannot exceed its predicted available output, ensuring system safety. The penalty terms  $-\delta_f (P_{f,t,z} - P_{f,t,pre})$  and  $-\delta_g (P_{g,t,z} - P_{g,t,pre})$  financially penalize any shortfall of actual renewable output from its predicted potential (i.e., curtailment). By minimizing the total cost  $F$ , the optimization is economically incentivized to drive  $P_{f,t,z} \rightarrow P_{f,t,pre}$  and  $P_{g,t,z} \rightarrow P_{g,t,pre}$ , thereby maximizing renewable utilization within the safe operational bounds defined by the constraints.

The output of thermal power units is expressed as follows Equation 2:

$$U_{i,t} = \begin{cases} 1, & \text{on} \\ 0, & \text{off} \end{cases} \quad (2)$$

The operating cost is Equation 3:

$$C_{i,t} = a_i P_{i,t}^2 + b_i P_{i,t} + c_i \quad (3)$$

In the formula,  $a_i$  (\$/MW<sup>2</sup>),  $b_i$  (\$/MW),  $c_i$  (\$) are the cost coefficients,  $P_{i,t}$  denotes the active power output.

The start-up cost is expressed as Equation 4:

$$Y_i = \begin{cases} Y_{hi}, & T_{off} \leq X_{off} \leq T_{off} + H_{csi} \\ Y_{ci}, & X_{off} > T_{off} + H_{csi} \end{cases} \quad (4)$$

In the formula:  $Y_{hi}$  represents the hot start-up cost of the  $i$ th thermal power unit,  $Y_{ci}$  denotes the cold start-up cost of the  $i$ th thermal power unit,  $T_{off}$  is the minimum down time constraint,  $X_{off}$  represents the actual down time of the unit,  $H_{csi}$  is the cold start-up time of the  $i$ th thermal power unit.

### 2.2 Wind and photovoltaic power output

Wind power output (Equation 5):

$$P_t^w = \frac{1}{2} \delta \pi \rho R^2 v_t^3 \quad (5)$$

In the formula:  $P_t^w$  denotes the actual output of the wind turbine at time  $t$ ;  $\delta$  represents the efficiency of the wind turbine generator;  $\rho$  is the air density,  $R$  stands for the radius of the wind turbine blade,  $v_t$  is the wind speed at time  $t$ .

Photovoltaic power output (Equation 6):

$$P_t^s = [1 - \sigma(T_t - 25)] A_s \mu_s I_t \quad (6)$$

In the formula:  $P_t^s$  denotes the output of the photovoltaic unit at time  $t$ ;  $\sigma$  represents the temperature coefficient;  $T_t$  is the ambient temperature at time  $t$ ;  $A_s$  stands for the area of the PV panel;  $\mu_s$  is the nominal efficiency of the PV panel;  $I_t$  is the solar irradiance at time  $t$ .

In the day-ahead dispatch stage, the combination of hydropower and thermal power units is adjusted based on the load forecast, as well as the wind and photovoltaic power generation forecasts. The rated power output of PV, wind, and nuclear power is treated as "negative load", and economic dispatch is performed in accordance with the day-ahead forecast values.

According to the priority of different objectives: The top priority is to minimize wind and PV curtailment, ensuring that all power

generated by wind, PV, and nuclear units is integrated into the grid. If the combined output of these three (wind, PV, nuclear) fails to meet the system load demand, hydropower units will be activated to supplement power generation and participate in dispatch. Only when the supplemented hydropower output still cannot satisfy the user demand will thermal power units be put into dispatch. This hierarchical dispatch logic aims to achieve the optimal economic efficiency of the system.

### 2.3 Thermal power and hydropower operation constraints

Equality constraints are as follows.

1. Constrained equilibrium equation:

In the dispatch problem of power systems, equality constraints are used to ensure the balance between power supply and demand. Specifically, the total output generated by all generators must match the real-time load demand of the power grid. This means the total electrical energy produced by the combined operation system must be equal to the total electrical energy consumed. The formula is as follows Equation 7:

$$\sum_{i=1}^{N_f} U_{i,t} P_{i,t} + \sum_{g=1}^{N_g} P_{g,t} + \sum_{s=1}^{N_s} U_{s,t} P_{s,t} + \sum_{f=1}^{N_f} P_{f,t} + \sum_{h=1}^{N_h} P_{h,t} + \sum_{ph=1}^{N_{ph}} U_{ph,t} P_{ph,t} = D_t \quad (7)$$

In the formula,  $t = 1, 2, \dots, T$ ,  $D_t$  denotes the grid load value at time  $t$ .  $P_{i,t}$  is thermal power,  $P_{g,t}$  is photovoltaic,  $P_{s,t}$  is hydropower,  $P_{f,t}$  is wind power,  $P_{h,t}$  is nuclear power,  $P_{ph,t}$  is pumped storage.

When  $P_{ph,t} < 0$ , pumped storage is in the state of pumped energy storage; When  $P_{ph,t} > 0$ , pumped storage is in the process of discharging water for power generation.  $U_{s,t}$  and  $U_{ph,t}$  respectively represent the states of hydroelectric and pumped storage units.

The balance equation of the hydropower plant is as follows.

2. Fixed head hydropower plant (Equation 8):

$$\sum_{t=1}^T q_k^t - l_k = 0, k \in \vartheta_W \quad (8)$$

In the formula,  $q_k^t = b_k (P_k^t)^2 + c_k P_k^t + d_k$ ,  $q_k^t$  is the flow rate of hydropower plant  $k$  in the  $t$ -th period,  $P_k^t$  is the output of that period,  $l_k$  is the water volume, and  $\vartheta_W$  represents the set.

3. Variable head hydropower plant (Equation 9):

$$r_k^{t+1} - r_k^t - j_k^t + q_k^t = 0, k \in \vartheta_B \quad (9)$$

In the formula,  $q_k^t$  represents the flow rate, and  $s_k^t$  represents the amount of abandoned water;  $j_k^t$  is the injection volume,  $r_k^t$  is the storage volume, and  $\vartheta_B$  is the set.

4. Water balance equation for cascade hydropower plants (Equation 10):

$$r_k^{t+1} - r_k^t + q_k^t + s_k^t - j_k^t - \sum_{i \in S_k^u} (q_i^{t-\tau_{ki}} + s_i^{t-\tau_{ki}}) = 0, k \in \vartheta_T \quad (10)$$

In the formula:  $\tau_k^t$  is the water flow delay time;  $S_k^u$  is the collection of reservoirs;  $j_k^t$  is the natural water flow injection amount and  $r_k^t$  represents the storage capacity;  $\vartheta_T$  represents a collection of hydroelectric power plants.

5. Power balance (Equation 11):

$$P_k^t - c_{1k} (r_k^t)^2 - c_{2k} (q_k^t)^2 - c_{3k} r_k^t q_k^t - c_{4k} r_k^t - c_{5k} q_k^t - c_{6k} = 0 \quad (11)$$

Among them,  $q_k^t$  is the flow rate corresponding to the hydropower plant;  $r_k^t$  represents the storage capacity of the reservoir;  $c$  represents the water consumption coefficient of the substation.  $P_k^t$  represents the power of the hydropower plant at the corresponding time.

6. Initial and Termination Conditions for Water Storage Capacity (Equation 12):

$$\begin{cases} r_k^1 = r_k^{int} = A \\ r_k^{T+1} = r_k^{fin} = A \end{cases}, k = S_T \quad (12)$$

In the formula,  $r$  represents the storage capacity of the reservoir, where  $int$  represents the initial value and  $fin$  represents the final value;  $A$  is a constant value.

The inequality constraints are as follows.

1. Hot standby constraint:

The power system must reserve sufficient reserve capacity, as follows Equation 13:

$$\sum_{i=1}^{N_f} U_{i,t} P_{i,t}^{max} + \sum_{s=1}^{N_s} U_{s,t} P_{s,t}^{max} - \sum_{i=1}^{N_f} U_{i,t} P_{i,t} - \sum_{s=1}^{N_s} U_{s,t} P_{s,t} \geq R_t \quad (13)$$

In the formula,  $P_{i,t}^{max}$  represents the maximum output of thermal power and  $P_{s,t}^{max}$  represents the maximum output of hydropower;  $R_t$  is the thermal reserve capacity of the power system during time period  $t$ .

2. Unit operation output constraint:

Power generation unit output constraints (Equation 14):

$$U_{i,t} P_{i,t}^{min} \leq P_{i,t} \leq U_{i,t} P_{i,t}^{max} \quad (14)$$

In the formula,  $P_{i,t}^{max}$  is the maximum output, and  $P_{i,t}^{min}$  is the minimum output.

Output constraints of hydroelectric units (Equation 15):

$$U_{s,t} P_{s,t}^{min} \leq P_{s,t} \leq U_{s,t} P_{s,t}^{max} \quad (15)$$

3. Start stop time constraint:

In the power system, the state transition of the unit needs to follow a specific time interval, which is represented by the following (Equation 16):

$$\begin{cases} X_{on} \geq T_{on} \\ X_{off} \geq T_{off} \end{cases} \quad (16)$$

In the formula,  $X_{on}$  represents the time interval for continuous operation, and  $T_{on}$  represents the minimum value of the running time, and *vice versa*.

4. Climbing and descending slope constraint (Equation 17):

$$\max(P_{i,t}^{min}, P_{i,t-1} - DR_i) \leq P_{i,t} \leq \min(P_{i,t}^{max}, P_{i,t-1} + UR_i) \quad (17)$$

In the formula,  $UR_i$  represents the climbing rate, and  $DR_i$  represents the descending rate.

5. Flow restriction of hydropower plant (Equation 18):

$$q_i^t \leq \bar{q}_i^t \leq \bar{q}_i^t, i \in S_{W,B,T} \quad (18)$$

In the formula,  $q_i^t$  represents the lower limit of flow rate,  $\bar{q}_i^t$  represents the upper limit of flow rate, and  $S_{W,B,T}$  is the set of three types of hydropower plants.

6. Storage capacity limit (Equation 19):

$$r_k \leq r_k^t \leq \bar{r}_k, k \in S_{B,T} \quad (19)$$

In the formula,  $r_k$  and  $\bar{r}_k$  respectively represent the lower limit and upper limit of flow rate, and  $S_{B,T}$  is the set of variable head hydropower plants and cascade hydropower plants.

## 2.4 Nuclear power operation constraints

In regular operations, nuclear power plants typically operate at full load to provide base load. As long as the power reduction operation of nuclear power units is maintained within safe limits, the safe operation of the units can be ensured and the requirement for peak-shaving depth can be met.

According to relevant studies, the safe regulation range of nuclear power units is well-defined: during the first 80% of the nuclear power plant's operational lifespan, the units can safely adjust their output within the range of 50%–100% of the rated power. This flexibility enables nuclear power units to adapt to grid load changes while strictly adhering to safety constraints.

Among them,  $P_N$  is the rated power,  $P_{deh}$  is the amplitude of load reduction operation, and  $P_\Delta$  is the power during linear power up and down periods.

Operational constraints.

1. Peak shaving constraint (Equation 20):

$$P_{deh} \leq 50\%P_N \quad (20)$$

2. Speed regulation constraint (Equation 21):

$$\Delta P = \frac{P_{deh}}{T_{\Delta P}} \quad (21)$$

3. Low power constraint (Equation 22):

$$1 - \frac{P_{deh}T_{dh} + 2(P_N - P_\Delta)T_{\Delta P}}{TP_N} \geq \beta \quad (22)$$

In the formula,  $T_{dh}$  represents the time of operation under low power conditions;  $\beta$  is the load factor.

The expression for low-power running time is Equations 23, 24:

$$T_{dh} \leq \frac{(1 - \beta)TP_N - 2(P_N - P_\Delta)T_{\Delta P}}{P_{deh}} \quad (23)$$

$$P_n^t = \begin{cases} P_N^r - P_{deh}, t \leq T_{dn} \\ P_\Delta, t \in T_{\Delta P} \\ P_N^r, T_{dn} + T_{\Delta P} < t < T - T_{\Delta P} \end{cases} \quad (24)$$

In the formula,  $P_N^r$  represents the rated power, and  $P_n^t$  represents the output value.

The power adjustment process of a nuclear power plant is linear, and its output power shows a linear relationship with time, that is Equation 25:

$$P_\Delta = \begin{cases} P_{\Delta up} = \frac{P_{deh}}{T_{\Delta P up}} + P_N - P_{deh}, t \in [0, T_{\Delta P up}] \\ P_{\Delta dn} = P_N - \frac{P_{deh}t}{T_{\Delta P dn}}, t \in [0, T_{\Delta P dn}] \end{cases} \quad (25)$$

In the formula,  $P_{\Delta up}$  and  $P_{\Delta dn}$  respectively increase and decrease power output;  $t$  represents the time interval.

## 2.5 Constraints on pumped storage operation

1. Power constraint for water discharge and power generation (Equation 26):

$$P_{hmin} \leq P_{hi} \leq \min\left(P_{hmax}, \frac{E_i}{t} \eta_h\right) \quad (26)$$

2. Power constraint of pumped storage (Equations 27–29):

$$E_{i+1} = E_i + t\left(\eta_p P_{pi} - \frac{P_{hi}}{\eta_h}\right) \quad (27)$$

$$0 \leq E_i \leq E_{max} \quad (28)$$

$$P_{pmin} \leq P_{pi} \leq P_{pmax} \quad (29)$$

Among them,  $P_{hmax}$  represents the maximum power generation of the pumped storage power station (unit: MW), while  $P_{hmin}$  represents the maximum pumping power (unit: MW). The energy storage capacity of the upper reservoir of the pumped storage power station during period  $i$  is recorded as  $E_i$ . In addition,  $\eta_p$  represents the efficiency of pumped storage energy, and  $\eta_h$  represents the power generation efficiency under the discharge power generation mode.

## 3 RIME algorithm for day-ahead multi-energy scheduling

The day-ahead scheduling model for large-scale integrated new energy bases studied in this paper exhibits the following prominent characteristics:

High dimensionality of decision variables: It involves the on/off statuses and power outputs of dozens to hundreds of generating

units over multiple time periods. The high-dimensional nature of the problem stems from the large number of decision variables associated with multiple time cycles and generating units, rather than scenario-based uncertainty modeling.

**Highly nonlinear objective functions and constraints:** These include the quadratic cost curves of thermal power units, the head-flow-output relationships of hydropower units, the energy conversion efficiency of pumped storage systems, and the peak regulation constraints of nuclear power units.

**Inclusion of integer variables:** Referring to the binary on/off statuses of generating units.

**Complex and strongly coupled constraints:** Covering power balance, reserve requirements, ramp rate limits, water balance and cascade correlation of hydropower generation, energy states of pumped storage, and safe operation ranges of nuclear power units.

These characteristics categorize the problem as a MINLP problem, which leads to the following challenges: For large-scale cases, solution algorithms may encounter difficulties in solving the problem due to non-convexity, resulting in excessive computation time. In some instances, they may even fail to obtain a feasible solution or a high-quality optimal solution within an acceptable time frame. Traditional heuristic algorithms tend to get trapped in local optima in high-dimensional spaces, and their performance is highly sensitive to parameter settings (e.g., inertia weight). Their convergence accuracy and stability still need to be improved when dealing with strong constraints and complex nonlinearities.

To address the high-dimensional optimization challenges posed by the model, this paper adopts the RIME algorithm, which achieves efficient solution through its unique search mechanism. The Soft Rime Search Operator performs gradient-free, guided random exploration globally via adaptive parameters and random perturbations, effectively maintaining the diversity of the population in high-dimensional spaces and avoiding premature convergence. The Hard Rime Penetration Operator, based on fitness information, applies targeted perturbations to solutions, providing an effective means to escape from numerous local optimal traps in high-dimensional spaces. Meanwhile, problem-specific customizations—including hybrid encoding update rules for continuous and discrete variables, as well as an efficient constraint handling strategy that transforms complex constraints into penalty terms—enable the algorithm to avoid explicitly handling all constraint dimensions, significantly reducing the computational complexity of solving high-dimensional constrained problems. These mechanisms collectively ensure that RIME maintains robust search capability and convergence efficiency in the high-dimensional, strongly constrained mixed-integer nonlinear programming problem studied in this paper.

The RIME algorithm is an emerging intelligent optimization algorithm (Yulin, 2024) that simulates the formation process of rime in nature to solve the algorithm. The RIME algorithm consists of four steps: population initialization, soft rime search, hard rime puncture, selection and update.

### 3.1 Initialize the population

The rime population  $R$  is formed by  $n$  rime individuals, where each rime individual is composed of  $d$  rime particles, which serve as decision variables. In the RIME algorithm, a candidate solution

(called “frost ice individual”) represents a complete day ahead scheduling scheme. For a system consisting of  $N$  units with a scheduling period of  $T$  time periods, the solution is encoded as a high-dimensional vector  $X$ . As shown below (Equation 30):

$$X = [P_{th}, U_{th}, P_{hyd}, U_{hyd}, P_{nuc}, P_{wind}, P_{pv}, P_{ps}, U_{ps}]$$

$$R = \begin{pmatrix} x_{11} & \cdots & x_{1j} \\ \vdots & \ddots & \vdots \\ x_{i1} & \cdots & x_{ij} \end{pmatrix} \quad (30)$$

In the formula:

$P_{th}$ : Active output of thermal power units (continuous variable).

$U_{th}$ : Start stop status of thermal power units (0–1 variable).

$P_{hyd}, U_{hyd}$ : Output and status of hydroelectric units.

$P_{nuc}, P_{wind}, P_{pv}$ : Output of nuclear, wind, and solar power units (continuous variable, constrained by upper bound of predicted values).

$P_{ps}$ : The power of the pumped storage unit is positive for power generation and negative for pumping.

$U_{ps}$ : Operation mode of pumped storage unit.

$x_{ij}$  represents the  $j$  decision variable in the  $i$  solution.

### 3.2 Soft rime search

Soft rime search can efficiently traverse the solution space and suppress local optimal convergence by dynamically adjusting particle inertia weights and neighborhood search radii. The position of each rime particle is represented as Equation 31:

$$R_{ij}^{new} = R_{best,j} + r_1 \cos \theta * \beta * (h(Ub_{ij} - Lb_{ij}) + Lb_{ij}) \quad (31)$$

In the formula,  $R_{ij}^{new}$  is the updated position,  $R_{best,j}$  is the optimal rime particle,  $r_1$  is a random number between  $-1$  and  $1$ , and  $\cos \theta$  varies according to the number of iterations.  $\beta$  is the environmental factor,  $h$  is a random number between  $0$  and  $1$ ,  $Ub_{ij}$  is the upper bound of space, and  $Lb_{ij}$  is the lower bound of space.

Among them,  $\cos \theta$  and  $\beta$  change with the number of iterations, as shown in the following (Equations 32, 33):

$$\cos \theta = \pi \frac{t}{10T} \quad (32)$$

$$\beta = 1 - \left[ \frac{wt}{T} \right] \div w \quad (33)$$

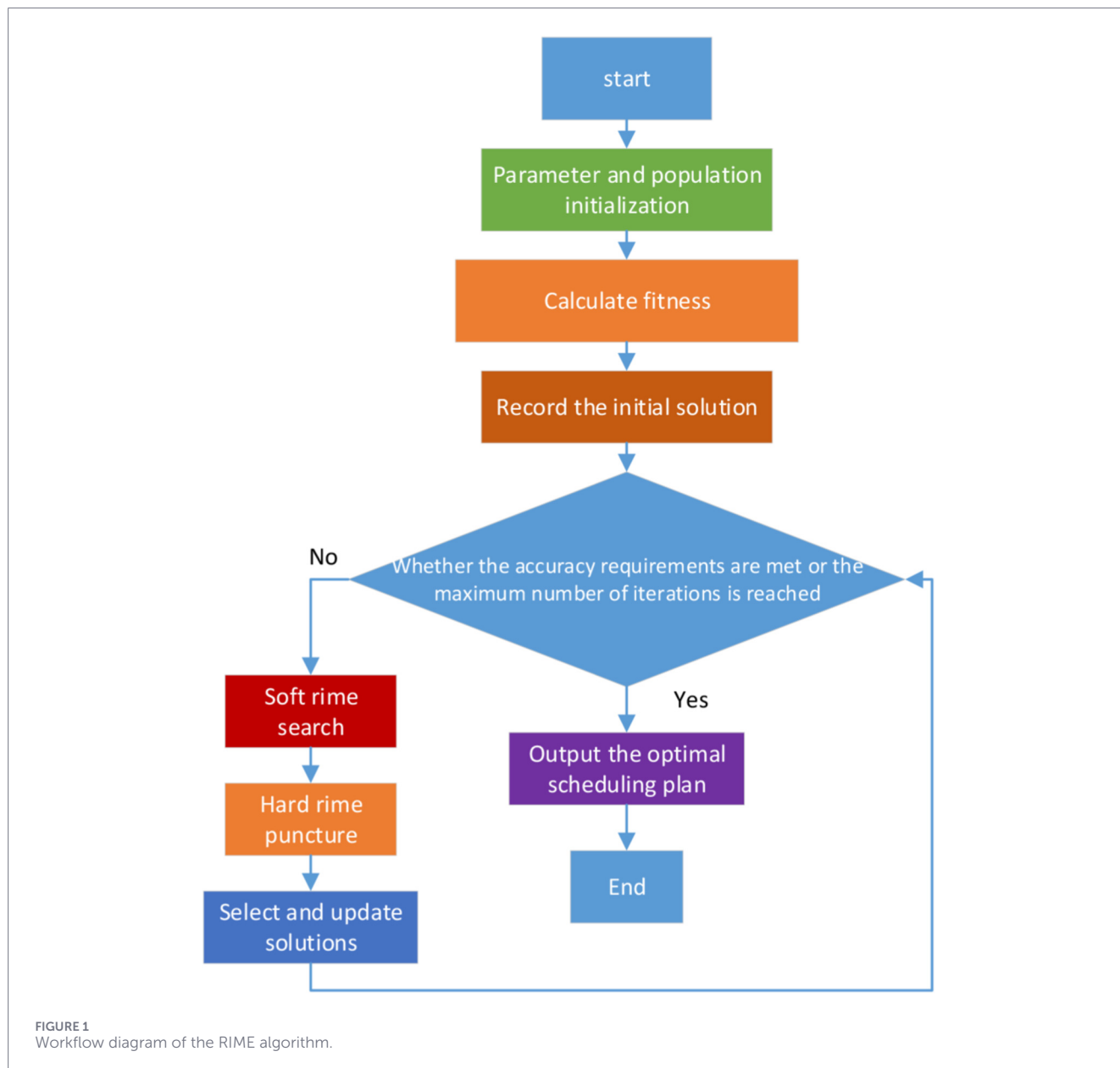
$t$  is the current iteration count,  $\left[ \frac{wt}{T} \right]$  represents the rounded value of  $\frac{wt}{T}$ , and  $w$  is the number of segments in the step function.

### 3.3 Hard rime puncture

The mechanism of hard rime puncture can avoid falling into the global optimum, which is represented by the displacement of rime particles. The formula is as follows Equation 34:

$$R_{ij}^{new} = R_{best,j} \quad r_3 < F^{norm}(S_i) \quad (34)$$

In the equation,  $r_3$  is a random number between  $-1$  and  $1$ , and  $F^{norm}(S_i)$  is the normalized value of the fitness of the current solution.



### 3.4 Selection and update

The selection and update mechanisms in the RIME determine the algorithm's convergence speed and iterative solution process. Population iteration is achieved through fitness evaluation, greedy selection, and optimal solution guidance.

The implementation process is as follows: In each iteration, the generated new solutions undergo fitness evaluation, and those meeting the requirements are retained. Through a greedy selection mechanism, the new solutions are compared with the original solutions and simultaneously mixed with the current global optimal solution to form hybrid solutions; the optimal one among these is selected as the solution for the next-generation, accelerating the movement of the population toward a better solution region. After each iteration, the optimal solution of the current population is recorded, and used to guide the search in subsequent

iterative calculations, realizing dynamically guided solution seeking.

Via a closed-loop process consisting of fitness evaluation, greedy selection, and optimal solution guidance, the selection and update mechanisms achieve global exploration and local optimization.

The core mechanisms of the RIME offer a novel approach to addressing the aforementioned challenges, specifically as follows: **Soft Rime Search:** This mechanism dynamically adjusts parameters and integrates random perturbations to effectively simulate the random growth process of ice crystals in a supercooled environment. It endows the algorithm with robust global exploration capability, facilitating the rapid localization of promising regions within a vast solution space, reducing the risk of trapping in local optima, and is particularly suitable for handling high-dimensional problems. **Hard Rime Piercing:** Based on fitness, this mechanism performs "piercing" updates on particles, simulating the abrupt growth of ice

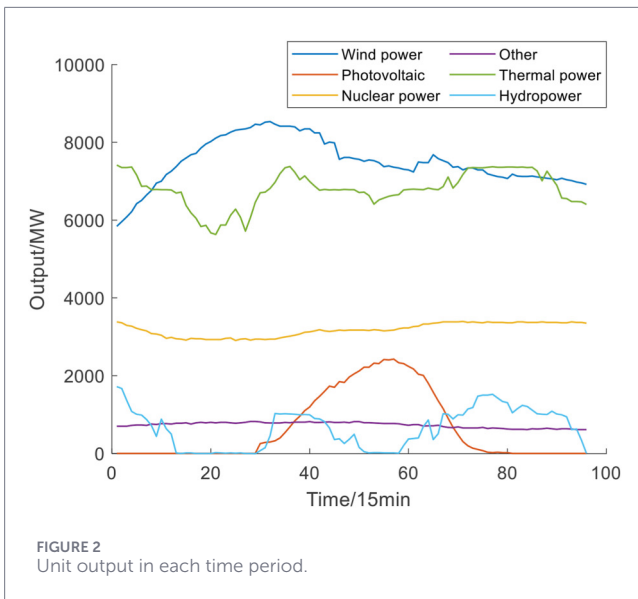


FIGURE 2  
Unit output in each time period.

crystals under specific conditions. It provides an effective means to escape local optima and enhances the algorithm's optimization performance in complex multimodal problems. Greedy Selection and Update: This mechanism accelerates the migration of the population toward regions with better solutions and improves convergence speed. It is crucial for engineering problems that demand high-quality solutions within a limited timeframe (e.g., the computational time window for day-ahead dispatch). Algorithm Structure: RIME features a relatively concise workflow and requires few parameters (primarily including population size, maximum number of iterations, and number of step function segments), making it easy to implement and adjust.

Therefore, this paper selects the RIME to solve the complex dispatch problem of hybrid energy bases. The aim is to leverage its superior global search capability, efficient local exploitation capability, robust constraint handling performance, and fast convergence speed to overcome the shortcomings of existing methods and seek a more economical and reliable dispatch scheme.

Solution representation: Each candidate solution (i.e., a 'frost ice individual') encodes the complete scheduling scheme into a vector  $X$ . This vector contains continuous variables (such as the output of all units at all time periods) and binary variables (such as the start stop status of thermal, hydro, and pumped storage units). For a system consisting of over 470 units and a 24-h scheduling cycle (96 time periods), the total dimensions of decision variables exceed 45,000, forming a high-dimensional search space. Constraint Handling: We employ a penalty function method to manage the complex equality and inequality constraints (power balance, ramping, water balance, etc.). The augmented fitness function for evaluating a solution  $X$  is Equation 35:

$$F_{aug}(X) = F(X) + \lambda_p * Penalty(X) \quad (35)$$

where  $F(X)$  is the economic objective from Equation 1,  $Penalty(X)$  aggregates all constraint violations, and  $\lambda_p$  is a dynamic penalty coefficient. This guides the search toward feasible regions.

RIME algorithm steps applied to scheduling problems:

Population initialization: Randomly generate a set of solutions. For continuous variables, sample uniformly within their upper and lower bounds; For 0–1 variables, randomly generate 0 or 1. Subsequently, a fast heuristic repair program (such as priority based adjustment) is applied to meet key constraints such as minimum start stop time, in order to improve the quality of the initial population.

Soft rime search: For continuous variables in solution  $X$ , update according to the original RIME formula. For 0–1 variables, first convert the continuously updated values into probabilities through the Sigmoid function, and then perform random sampling to determine the new 0/1 state, that is Equation 36:

$$U_{i,t}^{new} = \begin{cases} 1 & \text{if } rand < \frac{1}{1 + e^{-R_{i,t}^{new}}} \\ 0 & \text{other} \end{cases} \quad (36)$$

Hard rime puncture: If the random number is less than the normalized fitness of the solution, the solution is perturbed. This article proposes a problem aware perturbation strategy: randomly select 1-2 time periods, and regenerate the output of randomly selected units within that period to a large extent, while ensuring that their state changes meet the minimum operating time constraint. This helps to break out of local optima related to unit combinations.

Selection and Update: Adopting greedy choices. If the  $F$  of the new solution  $X^{new}$  is better than the original solution  $X$ , then replace it. At the same time, retain the global optimal solution  $X_{best}$  from previous generations to guide the search.

Algorithm Workflow Summary:

Input: system parameters, RIME parameters.

Initialize: Generate a population of solutions within bounds, applying a quick repair to satisfy simple constraints (e.g., min up/down times).

Iterate until stopping criteria are met: Apply Soft Rime Search to update all variables. Apply Hard Rime Piercing to selected individuals.

Repair & Evaluate: Perform a fast repair and compute the augmented fitness  $F_{aug}$ .

Greedy Selection: Update the population by retaining solutions with better  $F_{aug}$ .

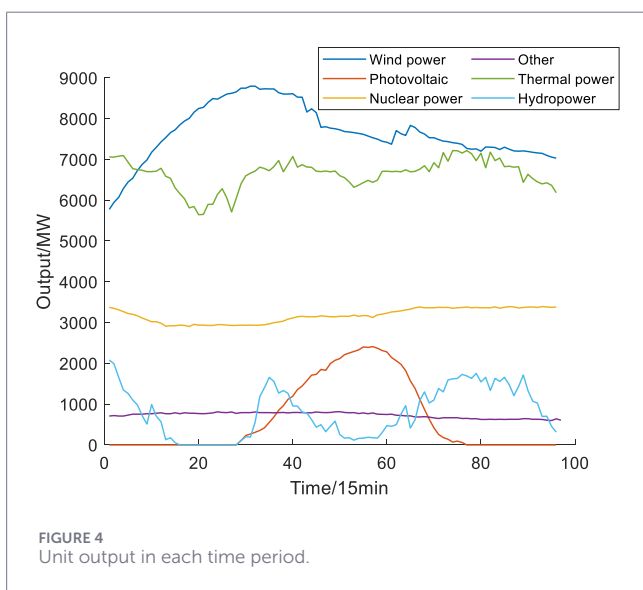
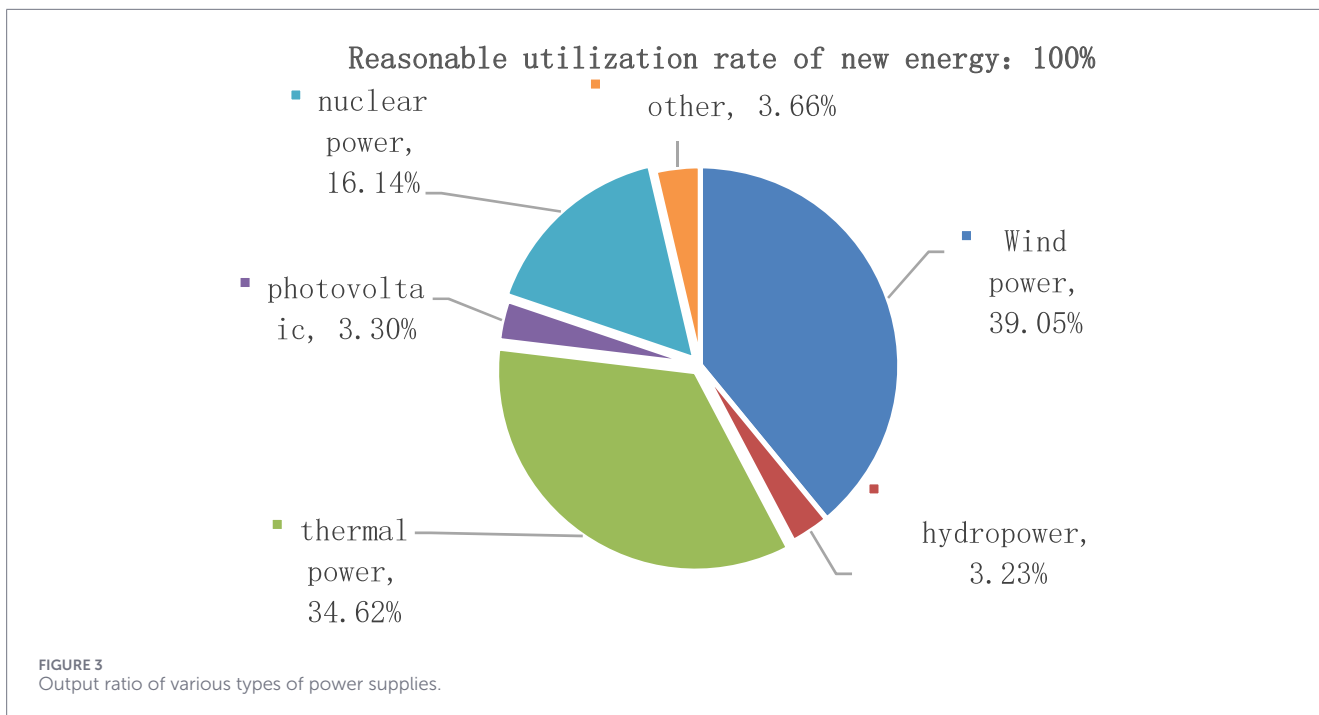
Output: The best-found dispatch schedule  $X^*$  and minimize costs  $F_{best}$ .

The RIME algorithm is used to solve the scheduling process of energy bases containing large-scale new energy, as shown in Figure 1.

## 4 Example analysis

This chapter applies the RIME algorithm to an energy base scheduling case involving large-scale new energy, optimizing unit output and rational utilization of new energy. Different scenarios are set up in the case to verify the rational utilization rate and optimal economic cost of new energy, and the cost and calculation time of different algorithms are compared to reflect the economic and practical results of the RIME algorithm.

The testing system is based on actual provincial cases and has high dimensions and complex constraints. The scheduling



problem poses a large-scale optimization challenge. This is mainly reflected in: the test system adopts a practical regional case, featuring high dimensionality and complex constraints that render the scheduling problem a large-scale optimization challenge. The total number of decision variables, including the continuous power outputs and binary operation statuses of all units across 96 time periods, reaches 71,520; Strong coupling: involving multiple types of strong coupling constraints such as hydropower cascade, pumped storage energy state, and nuclear power safety interval; Multimodal: The objective function and constraints are highly nonlinear. Therefore, this example is a representative testing platform for verifying the algorithm's ability to handle complex multi energy scheduling problems.

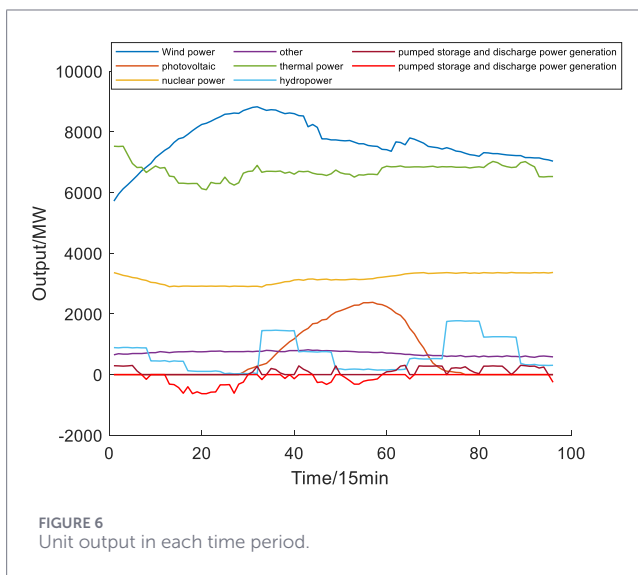
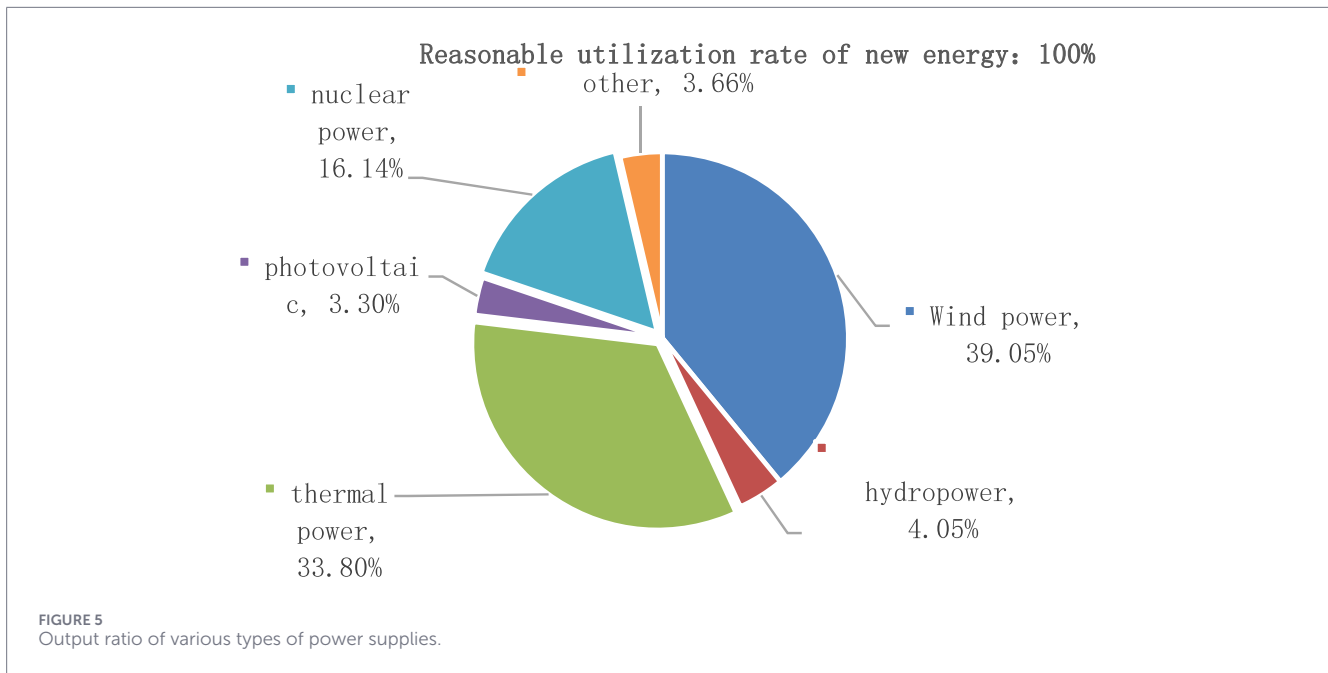
### 4.1 Recently optimized scheduling of energy bases containing large-scale new energy

Taking an energy base in a regional power grid as an example—this base integrates wind, photovoltaic, hydropower, thermal power, nuclear power, and pumped storage—it comprises 41 thermal power units, 141 hydropower units, 108 wind farms, 84 PV plants, 3 nuclear power units, and 93 units of other types. By optimizing the dispatch strategy of the energy base, the utilization rate of new energy is improved, and full-grid integration of new energy is achieved as much as possible to obtain the optimal economic benefits (Chen, 2019; Xintong, 2021). Meanwhile, it promotes the diversification of the base's energy structure, enhances the power system's new energy accommodation capacity, and realizes multi-energy complementarity (Xie, 2024). A model of this energy base is established (Guangxi Power Grid Co., Ltd., Guangxi University, 2023). To address the dispatch requirements of this region during the dry season, four operation modes are set up for output optimization analysis, thereby verifying the advantages of the RIME algorithm in solving the dispatch problem of large-scale new energy bases.

#### 4.1.1 Mode 1

Mode 1 allocates the output of hydroelectric units according to the planned electricity consumption. The unit output for each time period obtained by the RIME algorithm is shown in Figure 2.

As can be seen from Figure 2, the main power-generating units in the initial time period are wind power, thermal power, and nuclear power. Over the entire time period, the outputs of nuclear power and thermal power remain relatively stable. Among new energy units, wind power and PV power exhibit significant fluctuations—especially during the noon period, when PV output



reaches its peak. However, considering the need to maintain stable outputs of nuclear power and thermal power as much as possible, hydropower units participate in peak shaving to ensure the stability of the power system. The output proportion of each type of power source is shown in Figure 3.

As indicated in Figure 3, Mode 1 relies primarily on the output of wind power, thermal power, and nuclear power, accounting for 39.05%, 34.62%, and 16.14% respectively. The output proportion of hydropower is relatively small, and it is used for peak shaving to ensure the stability of the power system. Meanwhile, the rational utilization rate of new energy reaches 100%.

#### 4.1.2 Mode 2

Mode 2 allocates the output of hydroelectric units according to the incoming water volume. The RIME algorithm solves

the unit output of each time period in Mode 2 as shown in Figure 4.

As shown in Figure 4, wind power, thermal power, and nuclear power remain the main power-generating units. When the load demand increases, hydropower still serves as the primary unit for peak shaving to meet the load requirement. The output proportion of each type of power source is presented in Figure 5.

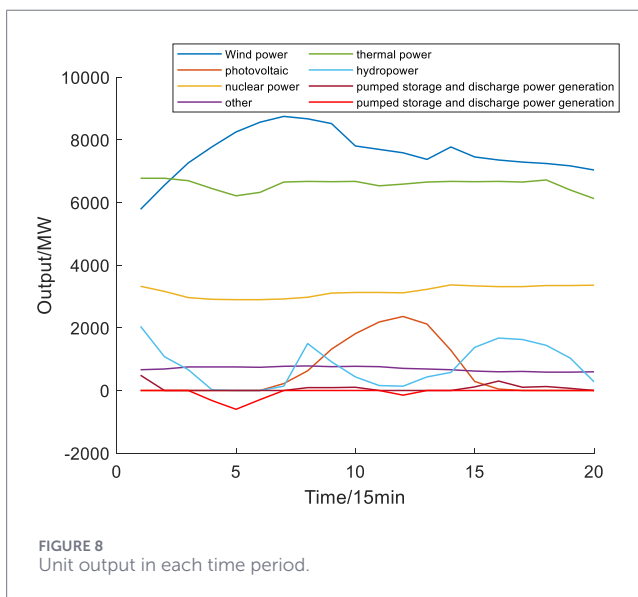
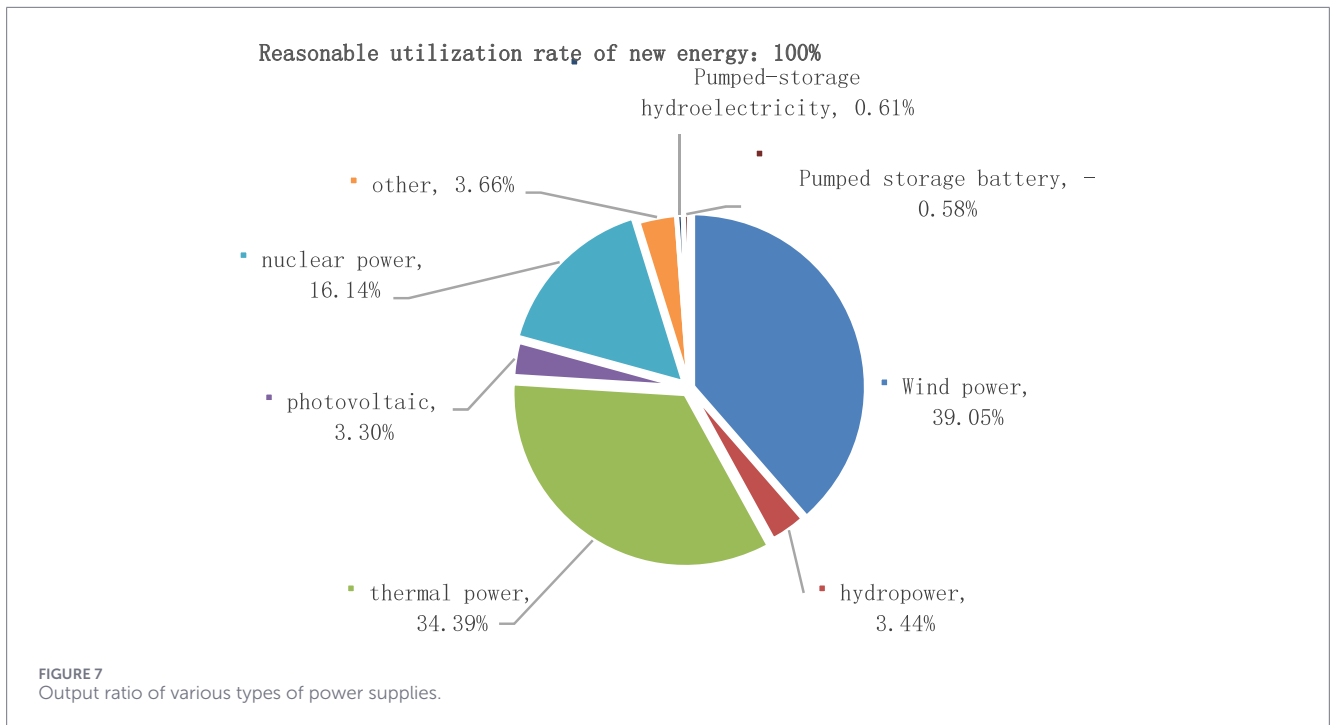
As observed in Figure 5, compared with Mode 1 (where hydropower output is allocated based on planned electricity quantity), Mode 2 increases the output proportion of hydropower units—from 3.23% to 4.05%—while reducing the output proportion of thermal power units, which decreases from 34.62% to 33.80%. Additionally, the rational utilization rate of new energy remains 100%, and the cost is reduced to a certain extent.

#### 4.1.3 Mode 3

Mode 3 considers the distribution of pumped storage energy according to the planned electricity output of hydroelectric units. Pumped storage has numerous advantages, such as peak shaving, frequency regulation, and black-start capabilities. Mode 3 demonstrates the output of hydropower units (with output allocated based on planned electricity quantity) and pumped storage units. This illustrates that the RIME algorithm not only delivers economic benefits in dispatch problems but also enables units to fully exert their functions of peak shaving and load leveling (peak clipping and valley filling).

After solving via the RIME algorithm, the unit output at each time period and the output of each type of power source are shown in Figures 6, 7, respectively.

Combined with Figures 6, 7, the main power output is concentrated in wind power and thermal power, accounting for 39.05% and 34.39% respectively. However, in addition to hydropower, pumped storage also plays a role in peak shaving.



The output process of pumped storage units exhibits significant complementary characteristics.

From the perspective of operation period distribution: Their power generation mainly occurs during daytime peak load hours and nighttime load peak periods, where they participate in power system peak shaving by connecting to the grid for power generation; Pumped storage operations (charging) are primarily scheduled during early-morning off-peak load hours, utilizing surplus power resources during this period for energy storage.

This period division strategy based on load characteristics can effectively smooth load fluctuations in the power system, reduce the impact of peak-valley differences on the safe and stable operation

of the power grid, and thereby improve the overall operational efficiency of the system. Meanwhile, under this operation mode, 100% full accommodation and efficient utilization of new energy can be achieved.

#### 4.1.4 Mode 4

Mode four considers the allocation of hydroelectric power output based on the amount of incoming water for pumped storage. Compared to Mode 3, considering pumped storage on the basis of Mode 2, the RIME algorithm was used to solve the unit output for each time period, as shown in Figure 8.

As can be observed in Figure 8, the system output is mainly borne by wind power and thermal power units, while hydropower and PV power primarily play a role in peak shaving. In addition, Mode 4 adopts a hydropower output allocation method based on incoming water volume. Compared with Mode 3—where pumped storage is also integrated under the same conditions and an electricity quantity allocation mechanism is used—Mode 4 enables more efficient utilization of water resources. The output proportion of each type of power source is shown in Figure 9.

As derived from Figures 3–9, the output proportion of hydropower units increases, rising from 3.44% (in Mode 3) to 4.05%, while the proportion of thermal power decreases from 34.39% to 33.79%, resulting in cost savings.

Through the calculation of the four modes, the output of each unit meets the demand, and the rational utilization rate of each unit reaches 100% in all cases. This indicates that the RIME algorithm can obtain the optimal solution, realizing maximum energy utilization, reducing the output of traditional energy sources, and improving the accommodation capacity of new energy.

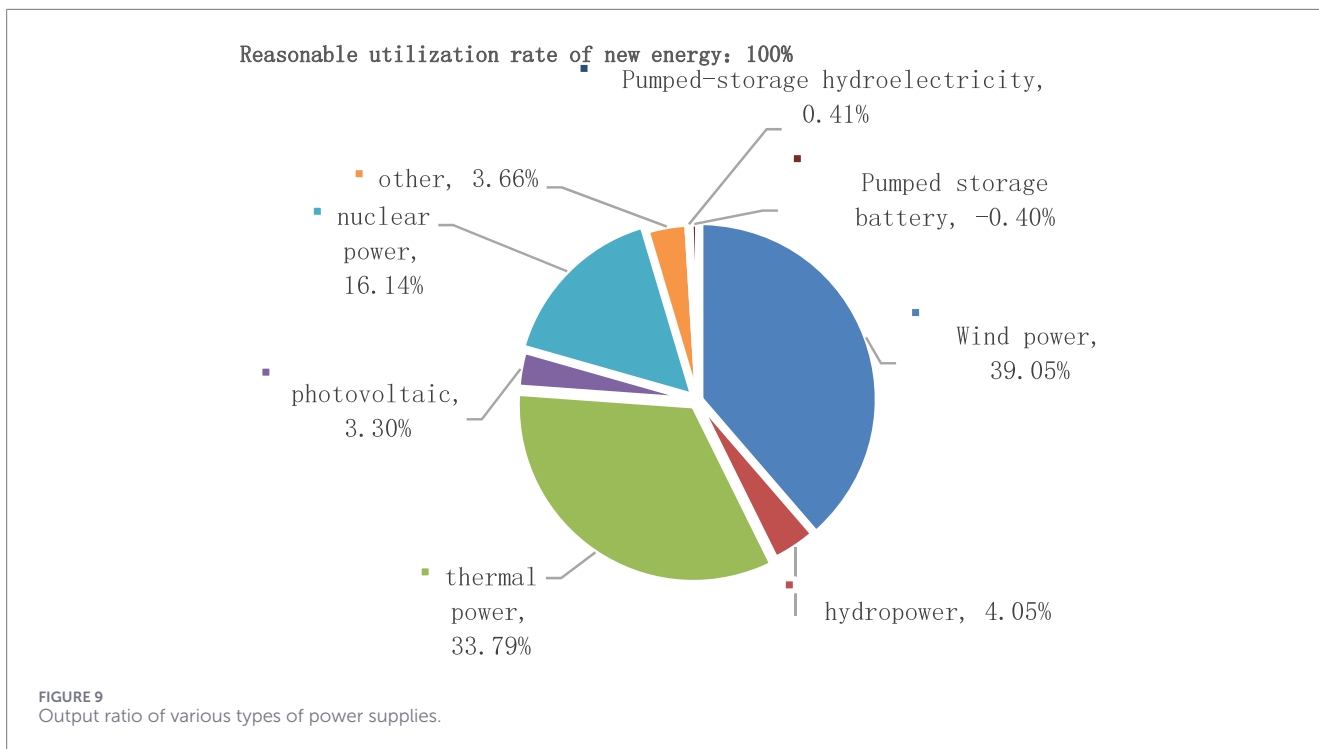


TABLE 1 Cost comparison between mode 1 and mode 2 algorithms.

| Algorithm | Mode 1 cost(¥) | Mode 2 cost(¥) |
|-----------|----------------|----------------|
| LR        | 6345072.079    | 6345072.079    |
| LS-MFA    | 6087341.437    | 6056377.465    |
| RIME      | 5710564.871    | 5748656.03     |

TABLE 2 Cost comparison between mode 3 and mode 4 algorithms.

| Algorithm | Mode 3 cost(¥) | Mode 4 cost(¥) |
|-----------|----------------|----------------|
| LR        | 6345072.079    | 6345072.079    |
| LS-MFA    | 6097347.476    | 6011379.951    |
| RIME      | 5792228.993    | 5713258.54     |

TABLE 3 Comparison of solution time of three methods.

| Mode   | LR      | LS-MFA  | RIME    |
|--------|---------|---------|---------|
| Mode 1 | 15.623s | 13.937s | 10.136s |
| Mode 2 | 90.764s | 89.657s | 84.786s |
| Mode 3 | 16.157s | 14.781s | 11.051s |
| Mode 4 | 93.367s | 91.975s | 85.887s |

## 4.2 Comparison of solving algorithms

The goal of energy base scheduling is to minimize the operating costs of the base and maximize the utilization of new energy generation, achieve economic scheduling, and thus minimize

operating costs to the greatest extent possible. In order to verify the advantages of the RIME algorithm in the scheduling problem of energy bases containing large-scale new energy, this paper compares and analyzes it with LR, which represents traditional mathematical programming methods, and LS-MFA, which represents heuristic algorithms.

The comparison of solution costs between Mode 1 and Mode 2 is shown in Table 1 below.

It can be observed that the cost calculated by the RIME algorithm is lower than those calculated by LR and LS-MFA. Specifically, compared with the LR method, RIME achieves a 10% cost optimization; compared with the LS-MFA algorithm, it achieves a 6% cost optimization. Moreover, Mode 2 further reduces the power generation cost by increasing the output of hydropower units.

In addition, based on Mode 1 and Mode 2, pumped storage is incorporated to form Mode 3 and Mode 4. Table 2 below presents the cost comparison between Mode 3 and Mode 4 (both considering pumped storage).

It is similarly observed that the cost calculated by the RIME algorithm is lower than those calculated by LR and LS-MFA. Specifically, RIME achieves a 10% cost optimization compared with the LR method and a 6% cost optimization compared with the LS-MFA algorithm.

In summary, the RIME algorithm yields the lowest cost across all four dispatch modes. Under all four modes, the RIME algorithm not only obtains the minimum total operating cost but also consistently ensures 100% new energy utilization (with no wind or photovoltaic curtailment). This fully verifies the superiority of the RIME algorithm in addressing the complex dispatch problem of hybrid energy bases—its strong global search capability and efficient constraint handling mechanism enable it to find feasible dispatch schemes that are closer to the global optimum or more optimal.

The comparison of solution times for the three methods is shown in [Table 3](#).

As shown in [Table 3](#), this study compares the solution times of LR, LS-MFA, and RIME across the four dispatch modes. The results indicate that: Across all four modes, the average solution time of RIME is only 84.7% of that of LR and 89.3% of that of LS-MFA. Particularly in complex scenarios such as Mode 2 (hydropower optimized by incoming water volume) and Mode 4 (incoming water volume + pumped storage), the solution time of RIME is as low as 84.786 s and 85.887 s, respectively—6.6% shorter than that of LR and 5.4% shorter than that of LS-MFA. The comparison of calculation time in [Table 3](#) shows that RIME maintains the highest computational efficiency in all four modes. It is worth noting that in scenarios where the coupling constraints of Mode 2 (water and electricity optimization based on incoming water) and Mode 4 (incoming water optimization + pumping storage) are more complex and the difficulty of solving significantly increases, RIME has a more significant advantage in computation time compared to LR and LS-MFA (saving about 6.6% and 5.4% respectively). This demonstrates the efficiency of the RIME algorithm mechanism in handling complex nonlinear coupling constraints.

RIME completes the large-scale dispatch solution (it comprises 41 thermal power units, 141 hydropower units, 108 wind farms, 84 PV plants, 3 nuclear power units, and 93 units of other types) within 10–85s, meeting the time-efficiency requirement of day-ahead dispatch. The coordinated improvement of its computational efficiency and optimization quality (6%–10% cost reduction) provides technical support for dispatch decision-making in energy bases with large-scale new energy integration.

## 5 Conclusion

This study demonstrates that the proposed RIME-based framework provides an effective, AI-driven solution to the computationally complex, high-dimensional day-ahead scheduling problem of renewable-rich multi-energy bases. Case studies on a realistically modeled regional system show that RIME can stably obtain superior economic solutions (6%–10% cost reduction) while ensuring 100% renewable utilization and maintaining computational efficiency. Its performance advantages are particularly evident in operation modes with intensified constraint coupling, underscoring its suitability for complex, large-scale optimization challenges.

The main contributions of this work are:

**AI-Driven Innovation:** We successfully applied RIME, a novel bio-inspired AI algorithm, to solve the complex MINLP problem associated with multi-energy scheduling. Its mechanisms—soft rime search and hard rime piercing—prove highly effective in maintaining global search capability and constraint satisfaction.

**Superior Performance:** Across four practical scheduling modes, RIME consistently outperformed traditional (LR) and heuristic (LS-MFA) methods, reducing operating costs by 6%–10% while ensuring 100% renewable energy utilization.

**Computational Efficiency:** RIME achieved significant time savings (10%–15% faster than benchmarks), making it suitable for real-world day-ahead scheduling applications.

**Sustainability Impact:** The energy base model is established and solved through the optimization of day ahead scheduling to maximize the use of new energy and achieve the goal of economic scheduling.

This study emphasizes the potential of artificial intelligence algorithms such as RIME in achieving intelligent, efficient, and sustainable clean energy systems. Future research will clearly focus on carbon emission costs or caps as the primary objective, with plans to develop a multi-objective RIME variant to simultaneously minimize operational costs and carbon footprint, thereby providing scheduling solutions that are more in line with strict 'dual carbon' policies.

## Data availability statement

The raw data supporting the conclusions of this article will be made available by the authors, without undue reservation.

## Author contributions

HZ: Writing – original draft, Writing – review and editing. LX: Conceptualization, Data curation, Formal Analysis, Funding acquisition, Investigation, Methodology, Project administration, Resources, Software, Supervision, Validation, Visualization, Writing – original draft, Writing – review and editing. ZH: Conceptualization, Data curation, Formal Analysis, Funding acquisition, Investigation, Methodology, Project administration, Resources, Software, Supervision, Validation, Visualization, Writing – original draft, Writing – review and editing. LB: Conceptualization, Data curation, Formal Analysis, Funding acquisition, Investigation, Methodology, Project administration, Resources, Software, Supervision, Validation, Visualization, Writing – original draft, Writing – review and editing. XD: Conceptualization, Data curation, Formal Analysis, Funding acquisition, Investigation, Methodology, Project administration, Resources, Software, Supervision, Validation, Visualization, Writing – original draft, Writing – review and editing.

## Funding

The author(s) declared that financial support was not received for this work and/or its publication.

## Acknowledgements

The authors would like to express their sincere gratitude to all the individuals and organizations that have supported this research.

## Conflict of interest

Authors HZ, LX, ZH, LB, and XD were employed by China Energy Engineering Guangxi Electric Power Design Institute Co., Ltd.

## Generative AI statement

The author(s) declared that generative AI was not used in the creation of this manuscript.

Any alternative text (alt text) provided alongside figures in this article has been generated by Frontiers with the support of artificial intelligence and reasonable efforts have been made to ensure accuracy, including review by the authors wherever possible. If you identify any issues, please contact us.

## References

- Bai, X., and Shahidehpour, S. M. (1996). Hydro-thermal, scheduling by tabu search and decomposition method. *IEEE Trans. Power Syst.* 11 (2), 968–974. doi:10.1109/59.496182
- Bai, J., Zhao, R., Xue, J., and etc, A. (2022). Photovoltaic gas synergistic unit combination model considering photovoltaic uncertainty. *Technol. Industry* 22 (11), 331–337.
- Chen, B. (2019). *Research on structural optimization method of offshore wind turbine triple pile foundation based on chaotic cloud GA and ANSYS [D]*. Harbin: Harbin Engineering University.
- Chen, G., Liang, Z., Gong, D., Zhu, G., Gong, D., Wei, H., et al. (2010). Optimal energy-saving dispatch of hydro-thermal power in Guangxi power grid based on interior point theory. *Guangxi Electr. Power* 33 (2), 1–4.
- Chen, G., Dong, Yu, and Liang, Z. (2020). Analysis and reflection on high-quality development of new energy with Chinese characteristics in energy transition. *Proc. CSEE* 40 (17), 5493–5506.
- Guangxi Power Grid Co., Ltd., Guangxi University (2023). Configuration method, system and storage medium for standby units: China, CN202310882499.2[P].
- Hua, W., Liang, Z., Yang, Y., Chen, G., Zhu, G., and Gong, D. (2010). Optimal coordination of fire, water and electricity in energy-saving dispatching. *Electr. Power Autom. Equip.* 30 (04), 1–4.
- Ke, Q. (2023). *Research on optimal dispatching strategy considering medium- and long-term contract electricity of concentrating solar power plant* (Doctoral dissertation). Chengdu: University of Electronic Science and Technology of China.
- Liu, N., Junjie, K., and Chunyang, Z. (2024). Development model and comprehensive benefit improvement method of multi energy complementary energy base. *Chin. J. Electr. Eng.* 44 (04), 1339–1352.
- Lu, R., Chen, D., and Hailei, H. (2023a). Method for supply-demand balance of water fire wind solar energy storage system based on heuristic unit combination algorithm. *Hydroelectr. Energy Sci.* 41 (11), 222–226.
- Lu, R., Chen, D., He, H., Zhang, S., Zhang, J., Zhang, Y., et al. (2023b). Supply-demand balance method for hydro-thermal-wind-PV-storage system based on heuristic unit commitment algorithm. *Water Resour. Power* 41 (11), 222–226.
- Qiu, J. (2021). *Economic dispatch of power system based on improved multidimensional firefly algorithm and differential evolution Black hole algorithm [D]*. Nanning: Guangxi University.
- Ren jundong research on optimization (2022). Ren jundong research on optimization of microgrid unit combination for new energy consumption by ren jundong. Hangzhou: Zhejiang University.
- Wang, Z. (2011). *Research on dynamic economic dispatch of power system with wind farms [D]*. Beijing: North China Electric Power University.
- Wong, S. Y. W. (1998). An enhanced simulated annealing approach to unit commitment. *Int. J. Electr. Power and Energy Syst.* 20 (5), 359–368. doi:10.1016/s0142-0615(97)00062-8
- Xie, X. (2024). *Study on location and capacity determination of centralized energy storage and optimal dispatching and control strategy of “double high” power grid [D]*. Nanning: Guangxi University.
- Xintong, L. I. (2021). *Cross-region optimal dispatch of power system considering spatiotemporal correlation of photovoltaic output [D]*. Jilin: Northeast Electric Power University.
- Yulin, L. I. (2024). *Reconstruction technology for photovoltaic-thermoelectric hybrid system based on improved rime algorithm [D]*. Kunming: Kunming University of Science and Technology.
- Zhang, Y. (2020). *Study on optimal dispatching strategy considering medium-term contract electricity of photothermal power station [D]*. Nanjing: Southeast University.
- Zhang, Y., Wu, F., and Zhang, S. (2023). etc robust unit combination model for photothermal power plants including CVaR. *Smart Electricity* 51 (10), 62–69.
- Zhou, B., Ning, C., Chen, S., Zhu, M., Su, Y., Zhou, Y., et al. (2024). Capacity planning and layout optimization method of wind-photovoltaic power stations in new energy base considering ecological resistance cost. *Electr. Power Autom. Equip.* 44 (7), 141–148.

## Publisher's note

All claims expressed in this article are solely those of the authors and do not necessarily represent those of their affiliated organizations, or those of the publisher, the editors and the reviewers. Any product that may be evaluated in this article, or claim that may be made by its manufacturer, is not guaranteed or endorsed by the publisher.